Resistivity of Mesopore Confined Solvent Free Ionic Liquid Determined by Electrochemical Impedance Spectroscopy of Ordered Porous Carbon Nanotube Supercapacitors

NanoFlorida 2020

Gibson Scisco

Dr. Mark E. Orazem

Dr. Kevin S. Jones

Dr. Kirk J. Ziegler

Approved for public release A: distribution is unlimited. 412TW-PA-20359

Supercapacitors

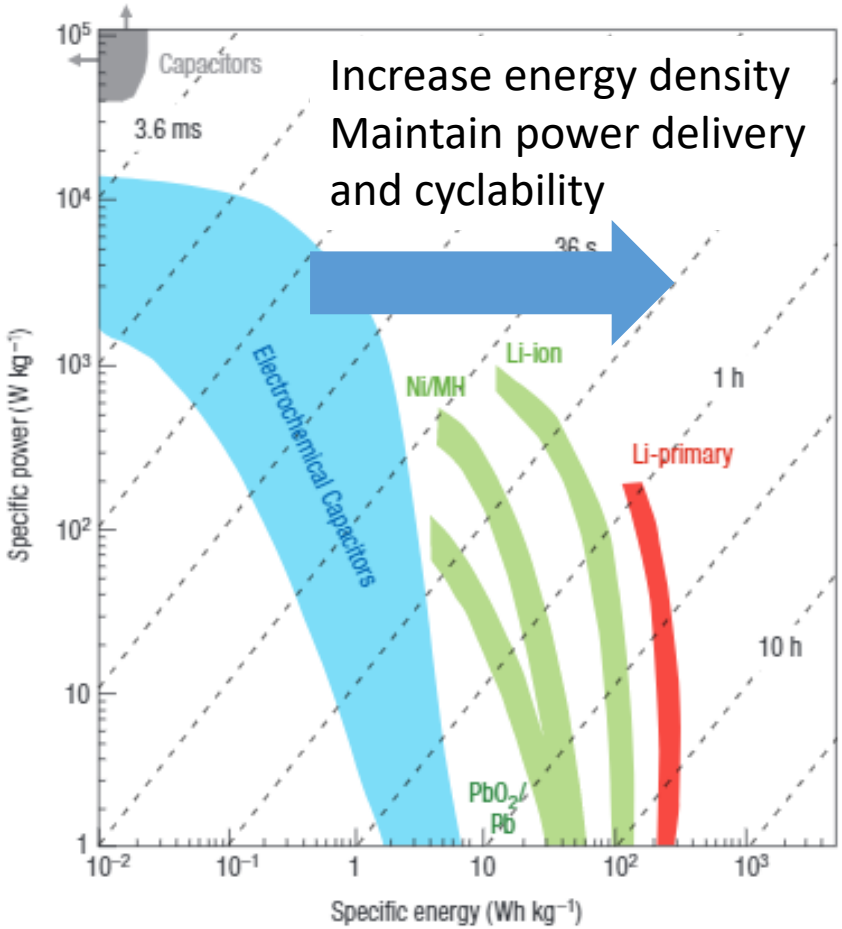

Increase energy density
Maintain power delivery
and cyclability

$$C = \frac{\epsilon A}{d} \qquad E = \frac{1}{2} C V^2$$

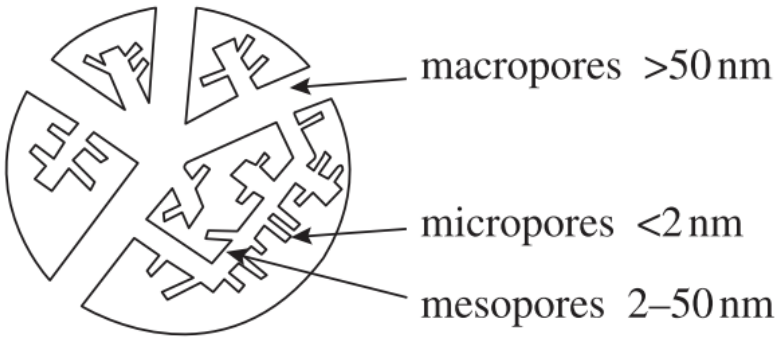

P. Simon and Y. Gogotsi, *Nat. Mater.*, vol. 7, pp. 845–854, 2008.
P. Simon and Y. Gogotsi, *Phil. Trans. R. Soc. A*, vol. 368, pp. 3457–3467, 2010

Ionic Liquids

- Organic salts
- Liquids at room temperature
- Suffer from low conductivity
  - ~50-100 Ω cm
- High electrochemical potential window of 3 – 6 V
- 1-ethyl, 3-methylimidazolium tetrafluoroborate (EMIM-BF4)
  - Bulk resistivity 70.9 Ω cm
  - ECW 4.7 V

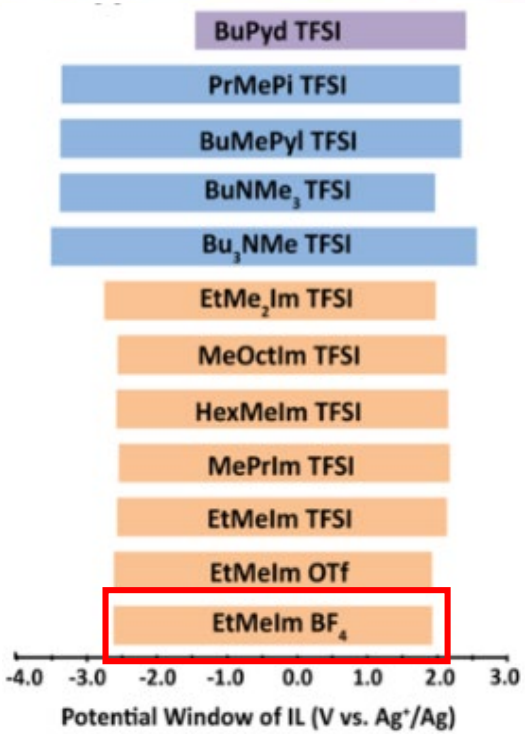

EtMeIm

BF_4

M. P. S. Mousaviet al., *ACS Appl. Mater. Interfaces*, 2016.

Nanopores Increase Capacitance

- Pores close to ion size, <1 nm diameter
- Decrease charge separation distance
- Higher capacitance per unit area of electrode

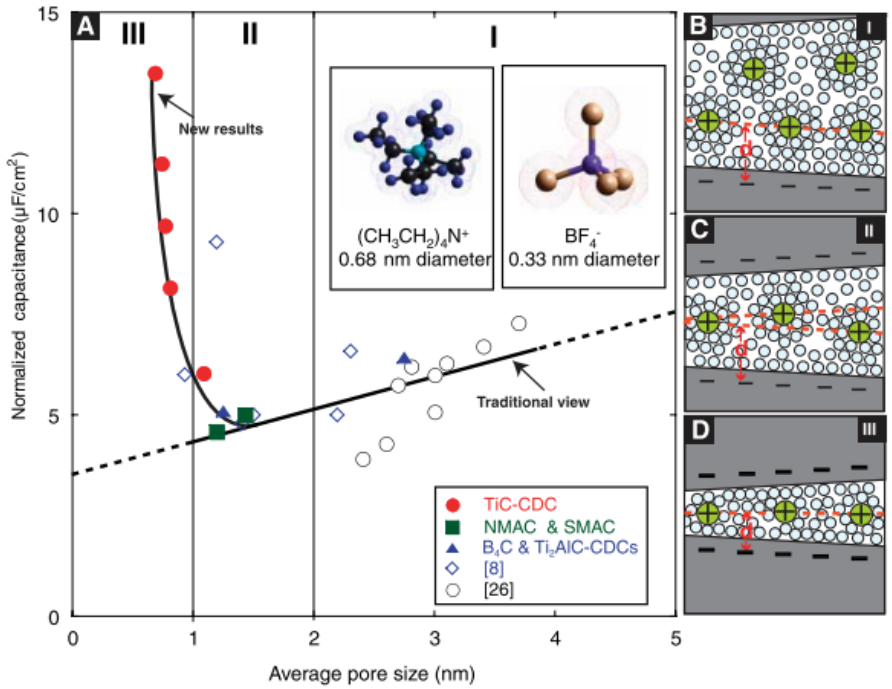

J. Chmiola et al., *Science*, vol. 313, pp. 1760-1763, 2006.

Nanopores Increase Resistivity

- BMIM-CH_3SO_4
- BMIM- $C_5H_{11}O_2SO_4$
- Current-Voltage measurements of individual conical nanopores
- Below 20 nm, resistivity greater than bulk

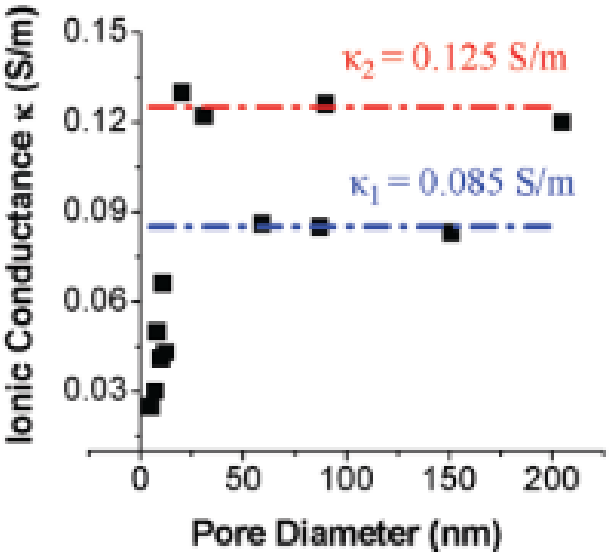

M. Davenport et al., *Nano Letters,* vol. 9, pp. 2125-2128, 2009.

- Dielectric spectroscopy of IL within SiO_2 nanopores 7.5 ± 0.7 nm
- Untreated (hydrophilic): 10-fold drop in diffusivity
- Silanized (hydrophobic): return to near-bulk values

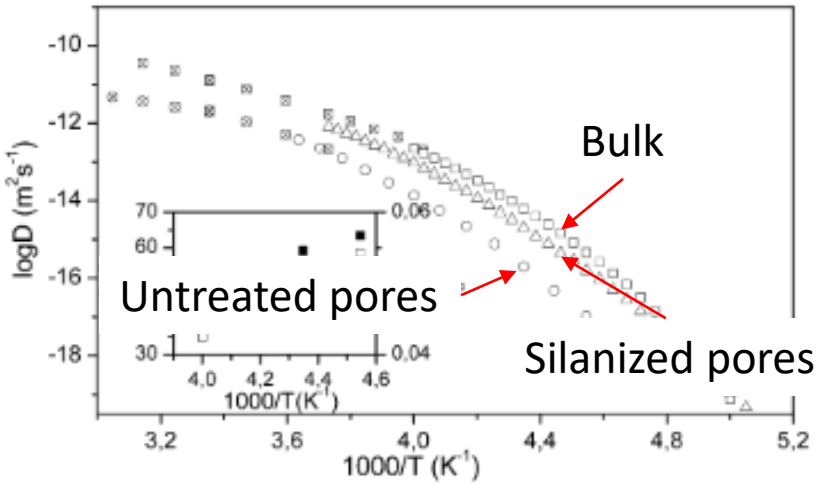

C. Iacob et al., *PCCP*, vol. 12, pp. 13798-13803, 2010.

Electrochemical Impedance Spectroscopy de Levie Model

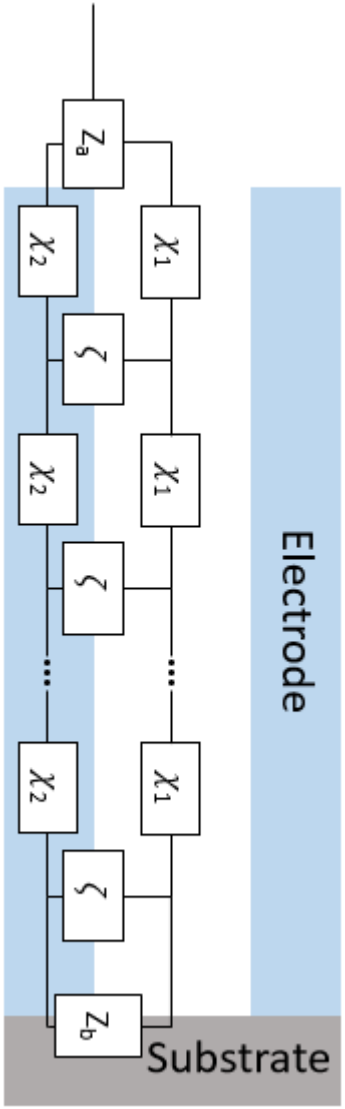

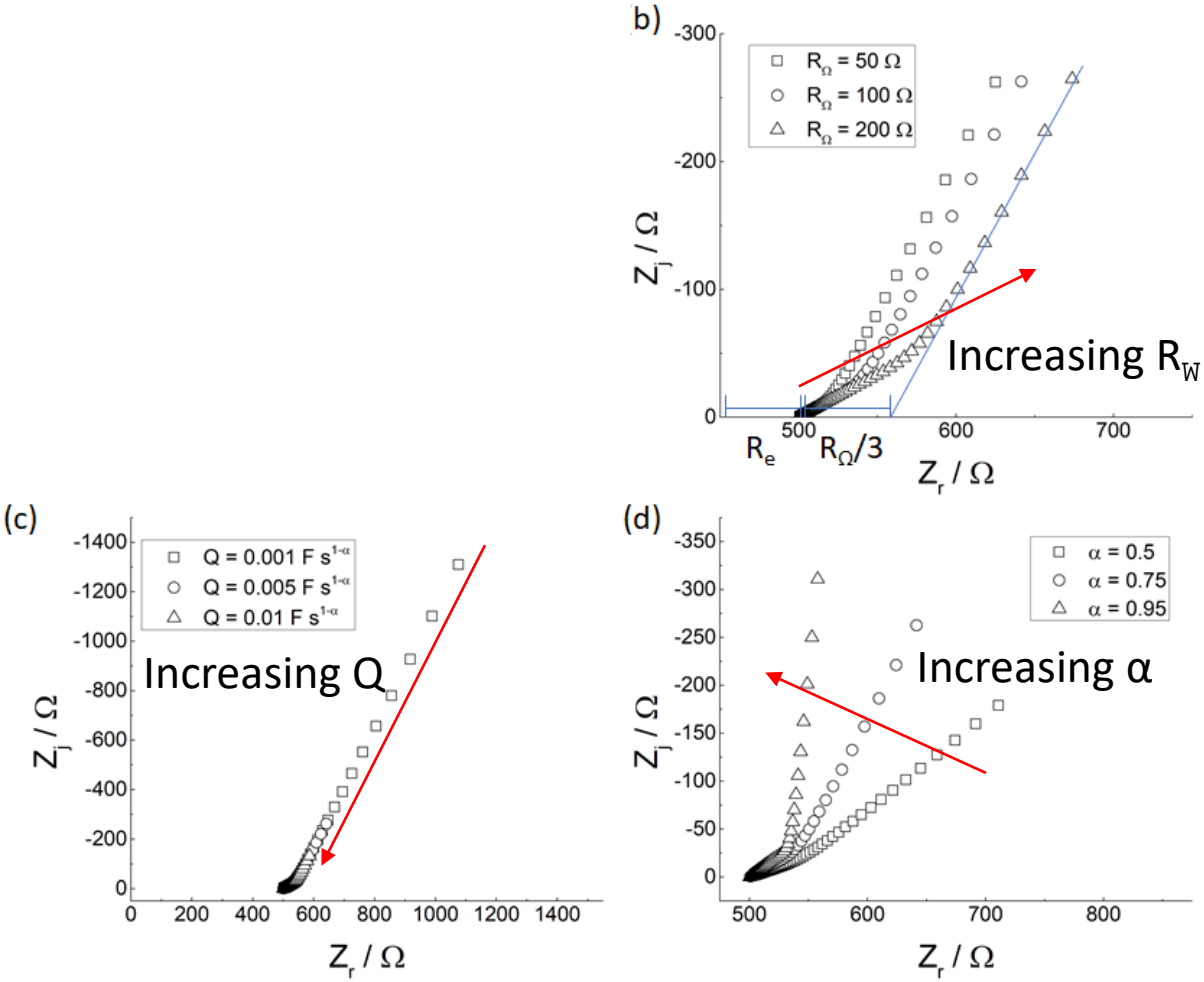

Electrochemical Impedance Spectroscopy de Levie Model

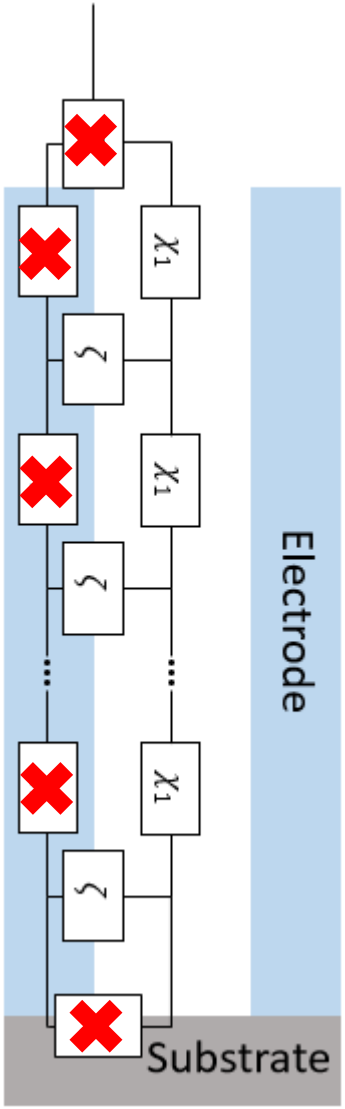

$$Z = R_e + \frac{R_\Omega}{\sqrt{\beta}}\coth\left(\sqrt{\beta}\right)$$

$$\beta = \frac{2n\pi r L R_\Omega}{(j\omega)^\alpha Q},\ R_\Omega = \frac{\rho_s L}{n\pi r^2}$$

$$\omega_{bp} = \frac{9r}{4\rho_s L^2 C_{sp}}$$

$$C_{sp} = Q^{\frac{1}{\alpha}}\left(R_e + \frac{R_\Omega}{3}\right)^{\frac{1-\alpha}{\alpha}}$$

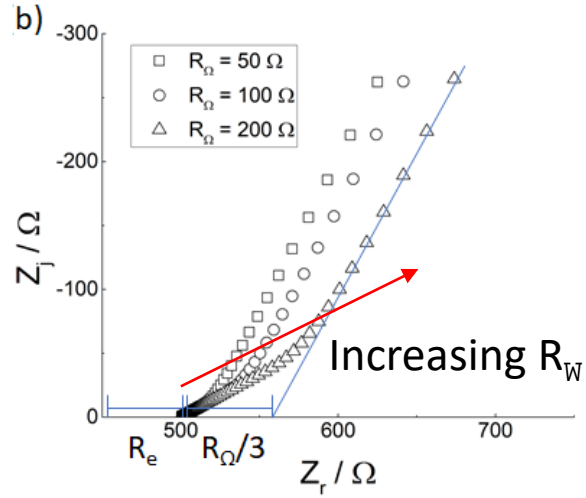

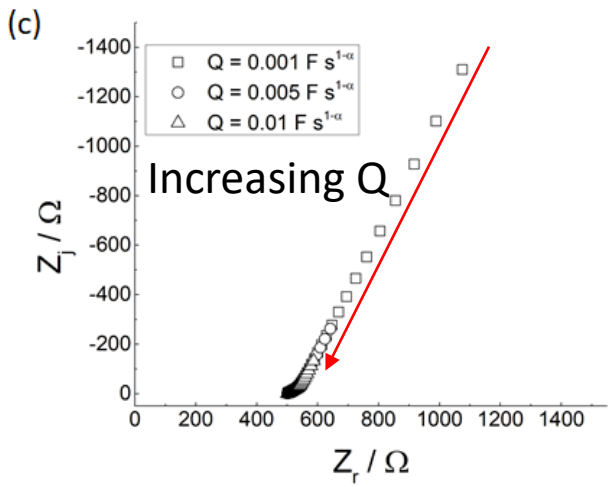

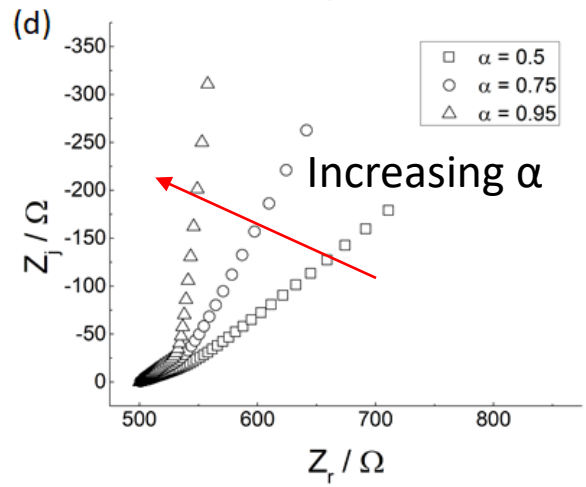

CNT-AAO Supercapacitors

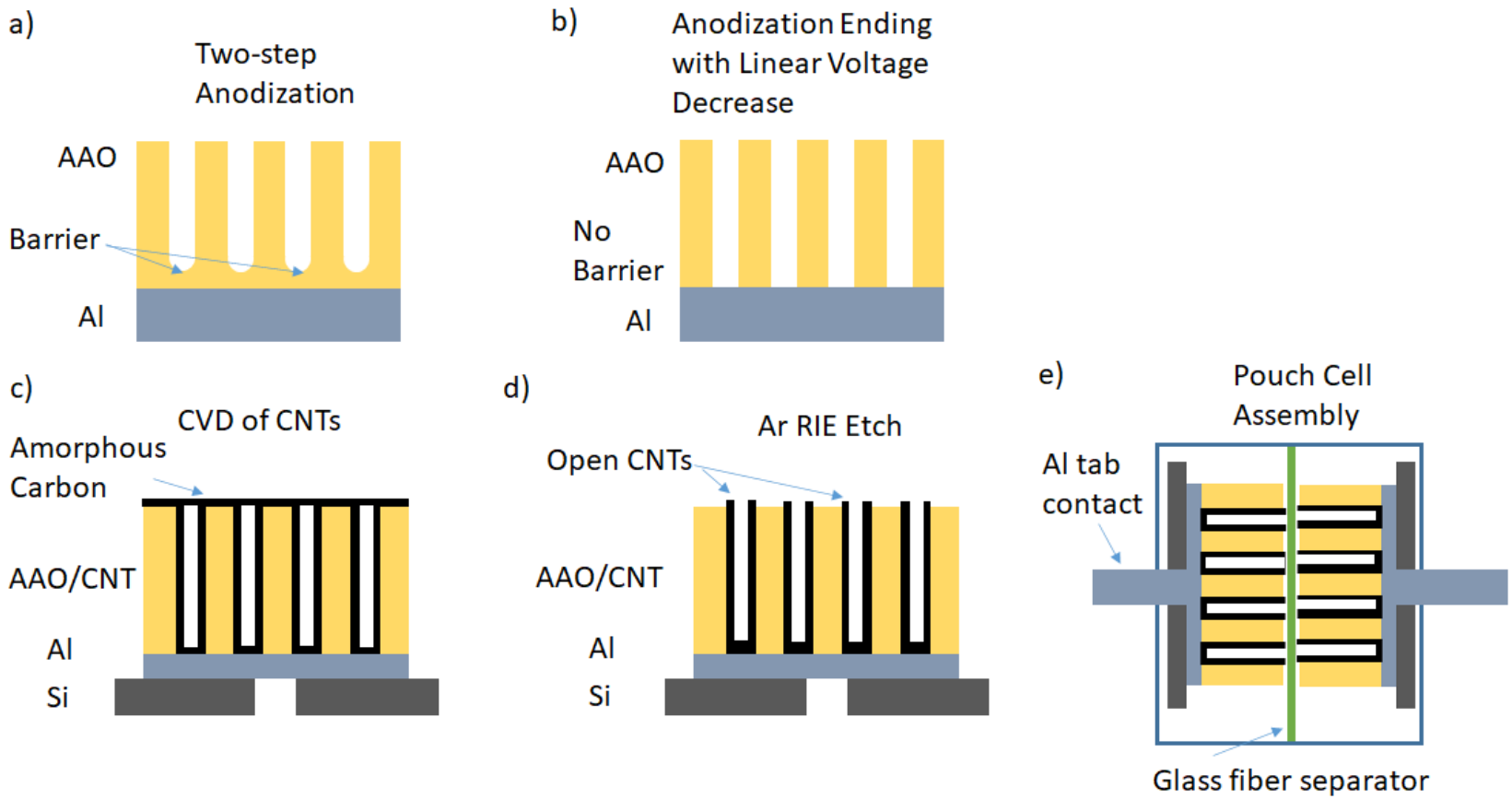

CNT-AAO Supercapacitors

Before CNT deposition
$D_p = 51 \pm 11$ nm
Pore density = 9.9×10^9 cm^{-2}

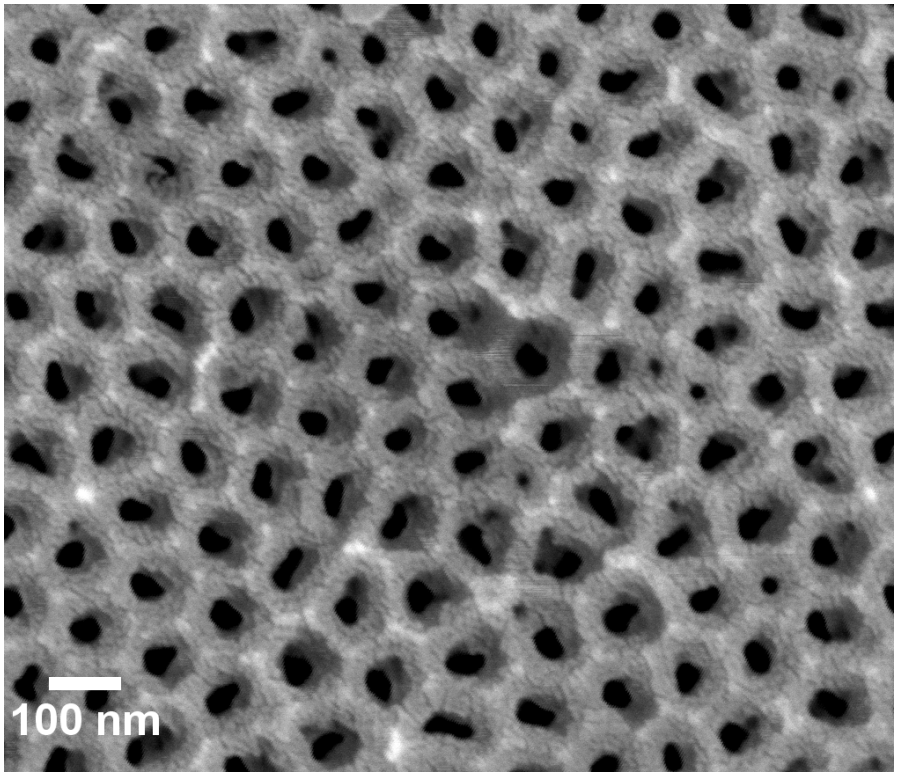

After CNT deposition
$D_p = 24.4 \pm 4.6$ nm
Pore density = 9.9×10^9 cm^{-2}

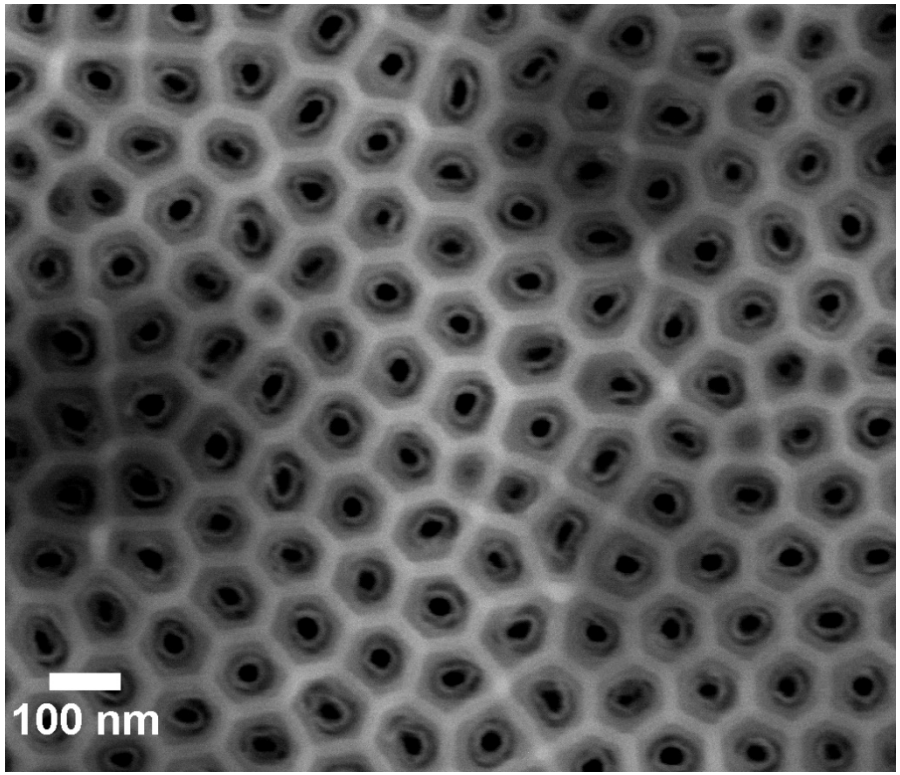

Control Flat Carbon

- Polished Al to P4000 grit and evaporated carbon to match CNT-AAO
- Roughness factor 1.12 determined by AFM
- Fit with R-CPE

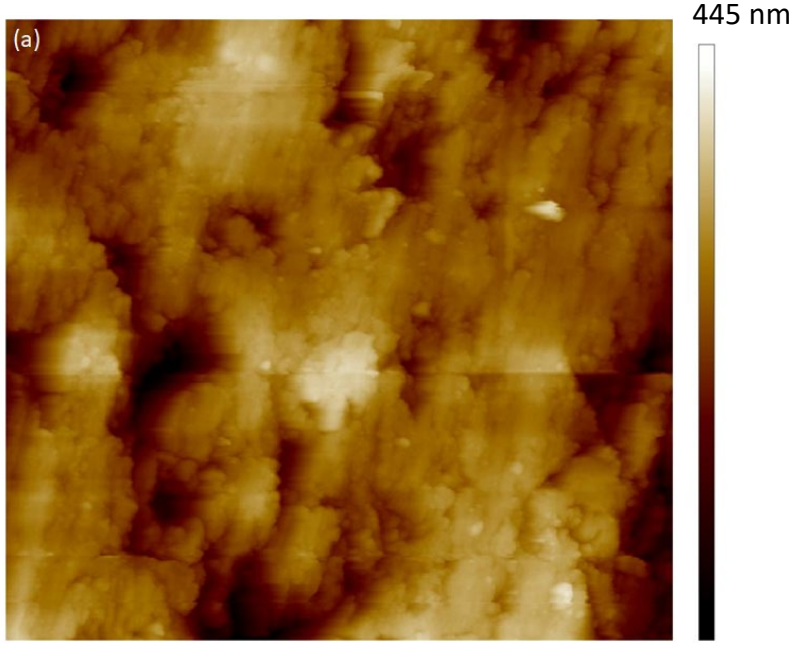

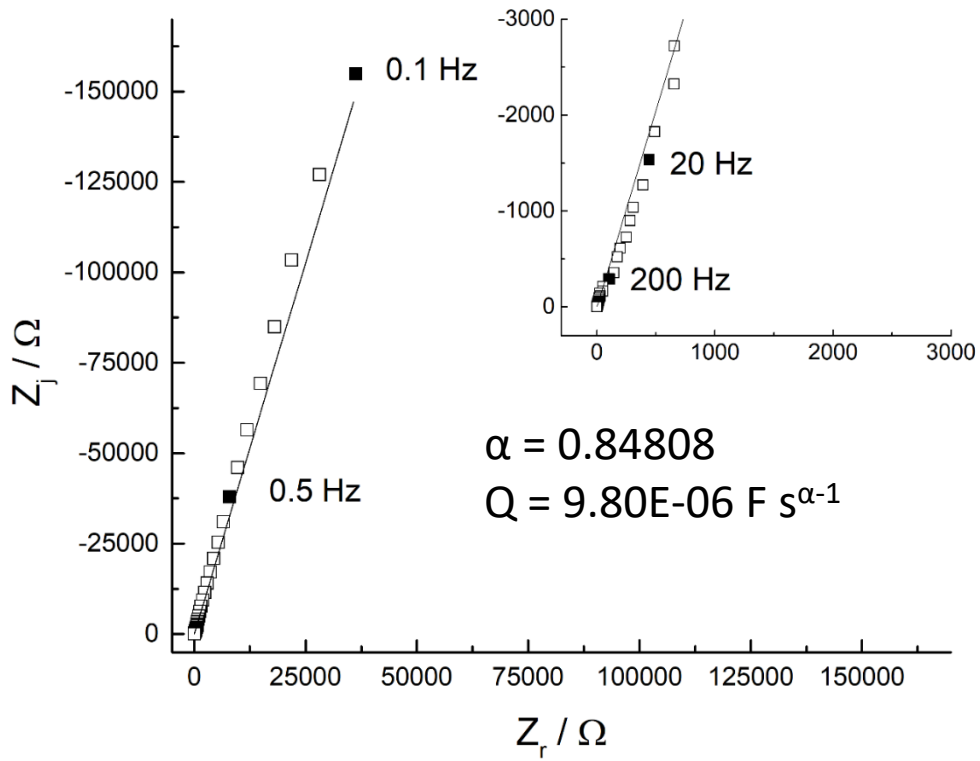

CNT-AAO Supercapacitors

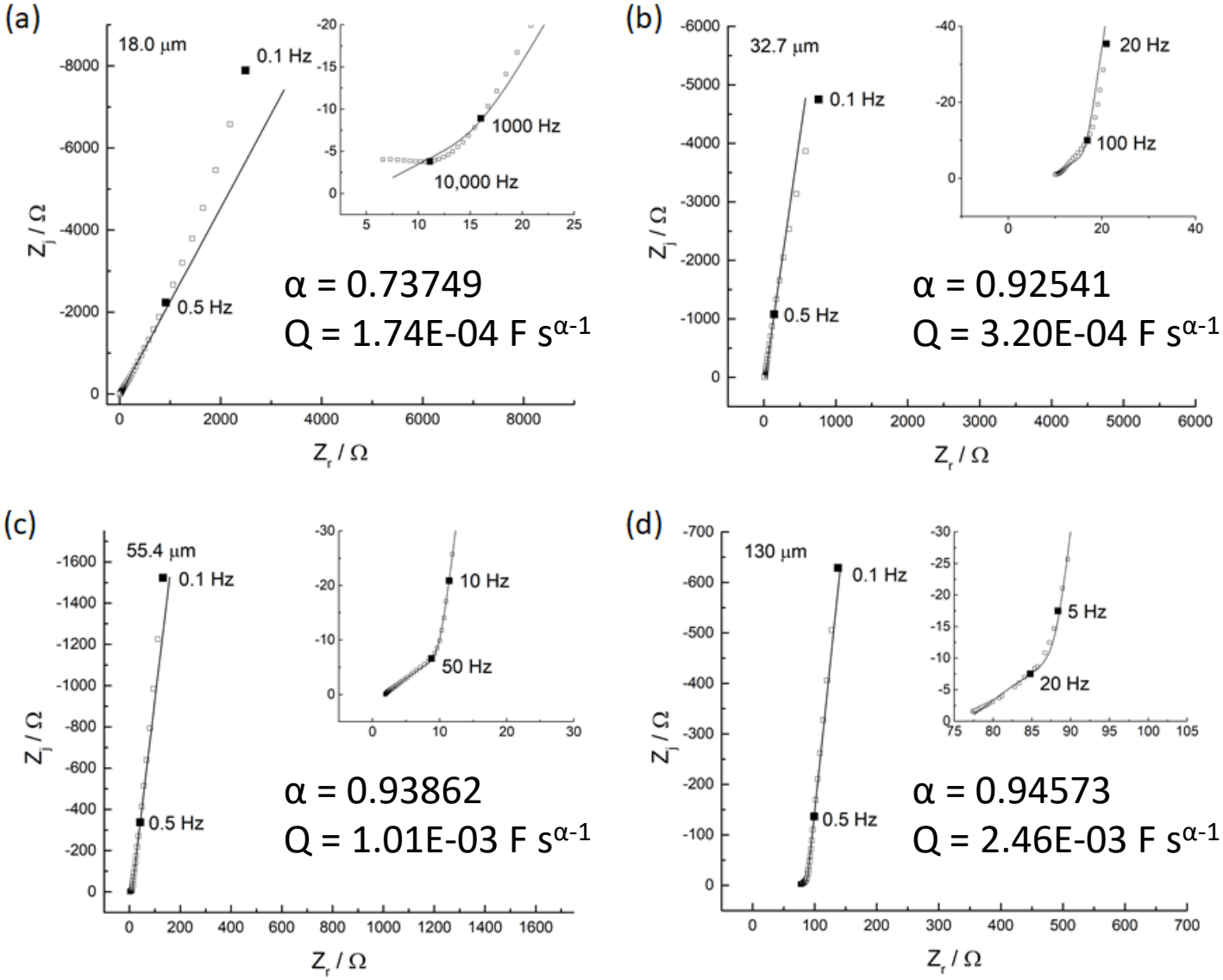

Ratio of Q Gives Ratio of Area

AAO Thickness [µm]	Q ratio	Q-derived Area [cm²]	Geometric Area [cm²]	Q/Geometric Area
Control	1.00	7.21	7.21	1
18.0	17.77	134.42	389.59	0.345
32.7	32.65	244.83	706.57	0.346
55.4	102.86	772.59	1197.44	0.645
130.4	251.37	1882.35	2820.99	0.667

- Q-derived area lower than expected based on pore dimensions and density
- Shift from ~35% to ~65% between 33 and 55 µm thick templates

TEM of CNTs

- ~30 µm template etched in NaOH, CNTs collected and imaged
- 5/32 (15.6%) tubes showed possible blockages
- Of these, 1 showed complete filling
- Blockages seemed more prevalent at ends – may be underrepresented

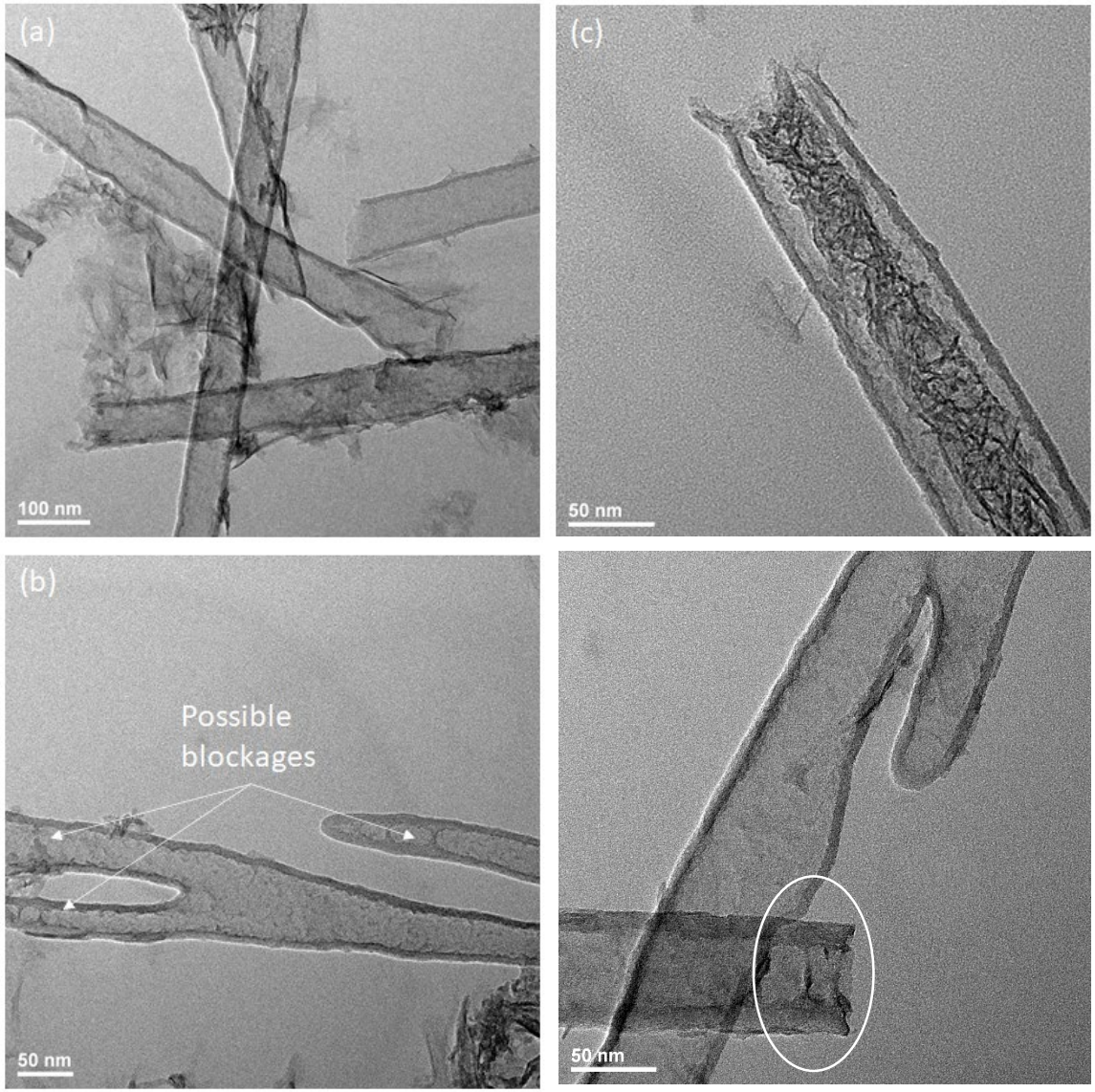

N_2 Adsorption BET

- AAO without CNT – 4 samples totaling 481 µm AAO
- AAO with CNT – 4 samples totaling 580 µm AAO

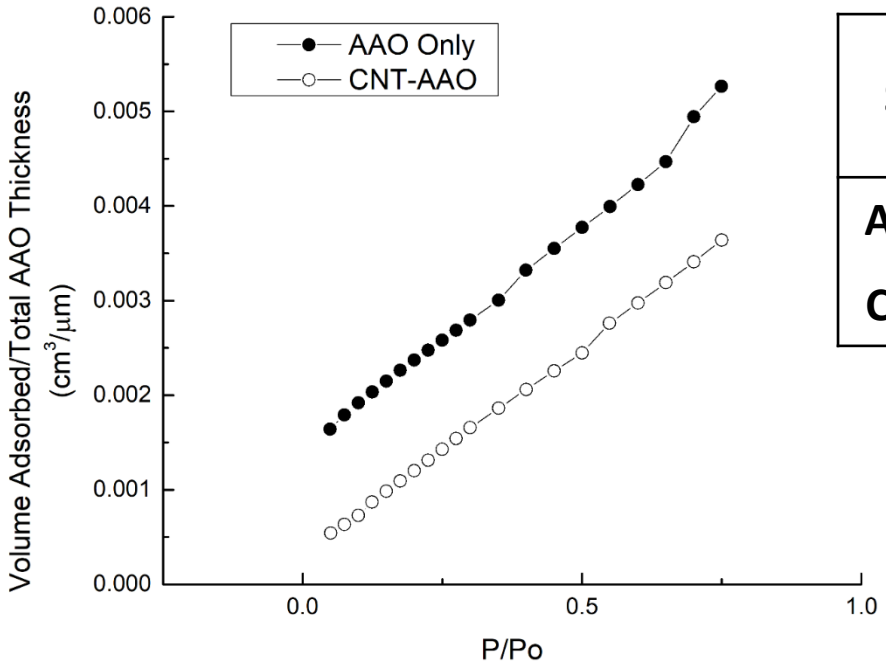

Sample	BET area [m²]	Geometric area [m²]	Ratio
AAO only	1.98	2.17	0.911
CNT-AAO	0.796	1.254	0.635

In-Pore Resistivity

- 399 ± 177 Ω cm
- 3 – 8x higher than bulk

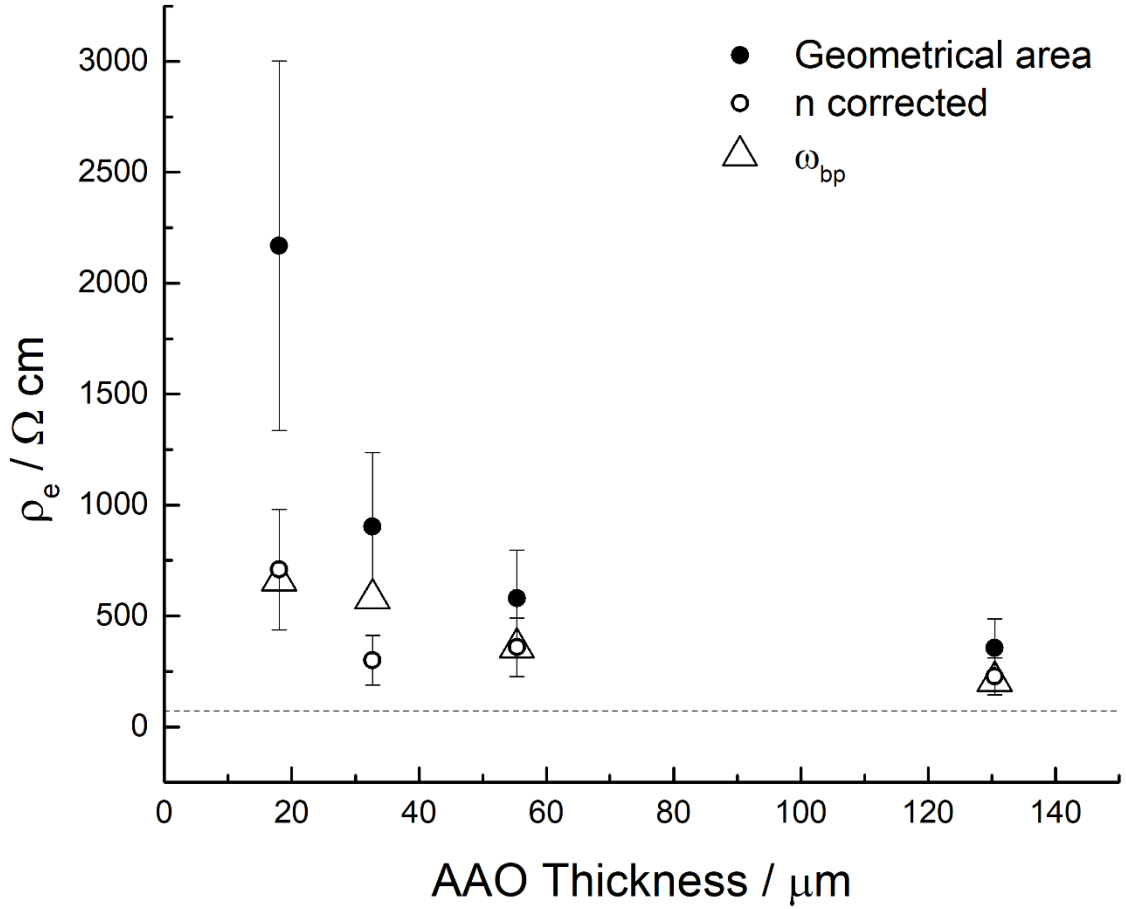

Conclusions

- CVD of CNT in AAO may not occur simultaneously on the pore wall as previously thought
  - Initiates at points on the wall with enhanced rates leading to blockages within the CNTs
  - Other blockages may be caused by complete filling of CNTs with carbonaceous material
- Blockages more prevalent in thinner AAO
  - CVD reaction determined by the reacting surface area
- Resistivity enhanced ~5 times in pores 25 nm in diameter
- Oxygen functional groups on surface of low temperature derived CVD carbon[1] may create hydrophilic/hydrogen bond inducing interface with IL

[1]P. Hou et al., *J. Mater. Chem.*, vol. 22, pp. 15221, 2012.